Towards the Prediction of Damage Of Peritectic Steels During Continuous Casting Process

C. Keller, R. Schwartz, M. Bobadilla, J. Tchoufang Tchuindjang, J. LecomteBeckers et al.

Citation: AIP Conf. Proc. **1353**, 151 (2011); doi: 10.1063/1.3589507
View online: http://dx.doi.org/10.1063/1.3589507
View Table of Contents: http://proceedings.aip.org/dbt/dbt.jsp?KEY=APCPCS&Volume=1353&Issue=1
Published by the American Institute of Physics.

Related Articles

New device to measure dynamic intrusion/extrusion cycles of lyophobic heterogeneous systems
Rev. Sci. Instrum. 83, 105105 (2012)

Non-destructive magneto-strain analysis of YB2Cu3Oy superconducting magnets using neutron diffraction in the time-of-flight mode
J. Appl. Phys. 112, 063923 (2012)

Energy exchange during slamming impact of an ionic polymer metal composite
Appl. Phys. Lett. 101, 094103 (2012)

Strain rate sensitivity and activation volume of Cu/Ni metallic multilayer thin films measured via micropillar compression
Appl. Phys. Lett. 101, 051901 (2012)

Microtensile testing of submicrometer thick functional polymer samples
Rev. Sci. Instrum. 83, 075110 (2012)

Additional information on AIP Conf. Proc.

Journal Homepage: http://proceedings.aip.org/
Journal Information: http://proceedings.aip.org/about/about_the_proceedings
Top downloads: http://proceedings.aip.org/dbt/most_downloaded.jsp?KEY=APCPCS
Information for Authors: http://proceedings.aip.org/authors/information_for_authors

ADVERTISEMENT

Towards the Prediction of Damage Of Peritectic Steels During Continuous Casting Process

C. Keller[a], R. Schwartz[a], M. Bobadilla[b], J. Tchoufang Tchuindjang[c], J. Lecomte-Beckers[c] and A.M. Habraken[a]

[a] *Department ArGEnCo, Division MS²F, University of Liege, Chemin des Chevreuils 1, 4000 Liege, Belgium*
[b] *Arcelor Research, BP 30320, 57283 Maizières-lès-Metz, France*
[c] *Department LTAS, Division MMS, University of Liege, Chemin des chevreuils 1, 4000 Liège, Belgium*

Abstract. In the Continuous Casting (CC) process, products are sometimes rejected or called defective due to the presence of transversal cracks. This type of macroscopic damage is expected to be due to a ductility loss during cooling in the bending and unbending areas of the CC line. In order to study this damage, a 2D model has been developed to predict at the mesoscopic level the intergranular crack event taking into account the creep and diffusion of voids. Already validated for a microalloyed steel, the model is identified and used in this study to predict the crack formation for three different grades of peritectic steels. Results show encouraging predictions of the damage. These latter, which depend on the chemical composition, are discussed in terms of microstructure and experimental device.

Keywords: Damage prediction, continuous casting, peritectic steels, finite element modelling
PACS: 46-62-81

INTRODUCTION

Continuous casting of steel became in recent years the first way to produce steel in large quantities. The technology and the production speed have quickly improved and the product quality has increased. So nowadays, to control this process in the best way, the comprehension of each process step and each material grade must be studied.

A relevant problem in the production of low carbon steels and stainless steels by continuous casting is the appearance of transverse cracks. During the process, the temperature of the steel decreases from the liquidus to the room temperature and crosses a very sensitive temperature range extending from 600°C to 1000°C where a strong loss of ductility generates a weakness of the material [1,2]. The brand reaches in general this sensitive temperature range in the unbending area [3] of the continuous casting mill and cracks can appear. These cracks, which are known to be intergranular [4], can be related to the steel grade but also to the mechanical and the thermal fields occurring during the process and to other factors such as the oscillations marks caused by the vertical oscillations of the mould. Moreover, the mechanical properties of steels at elevated temperatures are affected by several parameters, i.e. the temperature, the steel chemistry, the microstructure, the strain rate and the thermal history. Thus the correlation between the high temperature ductility and the crack susceptibility in continuous casting is not straightforward and must be properly studied to correctly predict the cracks occurrence for the critical steel grades.

Among the different steel families, peritectic steels seem to be very sensitive to the transversal crack formation. This steel family is usually employed for daily applications such as welded constructions or electric household appliances. For these materials, the chemistry and the microstructure, especially the nano-precipitates which form trend to dramatically enhance the crack formation. To optimize the continuous cast process and avoid the crack formation, the fracture mechanisms must be understood and predicted by a numerical model which takes into account both rheological and damage behaviour. The prediction of the damage is based on the microstructural

The 14th International ESAFORM Conference on Material Forming
AIP Conf. Proc. 1353, 151-156 (2011); doi: 10.1063/1.3589507

investigation of the material in order to introduce parameters which are linked to physical mechanisms of fracture (precipitate density, inclusion dimension and shape…)

The aim of this study is hence to identify and to employ a multi-scale model to predict the mechanical behaviour and the cracks formation during continuous cast for three different grades of peritectic steels. Firstly, the three grades of steels are analysed microscopically and the experimental device used to identify the model is described. Secondly, the multi-scale model is outlined with the macroscopic and the mesoscopic part. The model is then identified and used to predict the crack formation for the three steels. The results are finally discussed in terms of material microstructure and experimental procedure.

EXPERIMENTAL AND NUMERICAL STUDY

Description of the Material and of the Experimental Device

In an industrial point of view, the study of peritectic steels is fundamental because cracks appear on the surface of the slabs at the exit of the CC process. Due to the role played by the microstructure on the damage, it is important to choose different chemical compositions of peritectic steels in order to study more precisely the origin of the crack appearance. Among the steels of the peritectic family, three different grades were chosen for their different vanadium (V) and niobium (Nb) content (see Table 1). These two elements are involved in the precipitate formation which is detrimental for the material. The steel **Grade A** enables the study of the Nb precipitates effect on the damage. With the addition of V, the **Grade B** allows the study of this element on the crack sensitivity. Finally the steel **Grade C**, with large Nb and V contents enhances the study of both elements. Hence, the study of these steel grades enables the quantification of the precipitates influence on the crack appearance.

TABLE 1. Composition of the studied peritectic steel grades (in ppm)

Steel grade	C	Si	Mn	P	Ti	N	V	Nb	Al	S
Grade A	1790	3523	12149	80	37	58	1	161	403	8
Grade B	1748	183	14702	117	151	54	60	139	313	66
Grade C	576	2226	16220	119	163	45	20	668	396	24

The grain size and the precipitates, which are influent parameters on ductility, are taken into account for the damage prediction in FE model and must be properly characterized. Considering the austenitic grain size, scanning electron microscopy reveals, for a material with a microstructure representative of the original one at the beginning of the CC, that the mean value for the three grades is around 200 µm in agreement with others values [5,6]. The characteristics of the precipitates for the three grades were studied by Scanning Transmission Electron Microscopy (STEM). Table 2 summarizes the average diameter of the precipitates and their surface fraction computed from 10 analyzed grains for the three grades. For each grade, the precipitates are located around the old austenitic grain boundaries and in the grain interior as illustrated in figure 1(a). In agreement to its large contents in Nb and V, the **grade C** presents coarser precipitates than the two others grades together with a larger area fraction (more precipitates in the core of the grains). For the three grades, the investigation of the chemical composition of the precipitates by STEM showed that precipitates are mainly in the form TiNb(C,N) as illustrated in figure 1(b), in agreement with the chemical composition. However, surprisingly, no traces of V were found in the precipitates for the **grade B** and **grade C**.

TABLE 2. Results of the microscopic TEM analysis of the precipitates

Grade	Average diameter (nm)	Surface fraction (%)
A	30	0.06
B	30	0.059
C	50	1

To study the mechanical behavior of the material and to reproduce the mechanical loading that is experienced by the material during CC, Hot Tensile Tests (HTT) have been used. Among the different mechanical tests usually employed for CC modeling such as hot bending tests, compression tests…HTT allows an easy study of the transversal crack formation. To better identify the damage parameters of the model, the stress state was varied for

the tensile tests using notched specimens with 3 different notch radiuses (R=0; 2 and 4 mm). Different test temperatures were also chosen ranging from 700°C to 1100°C with different strain rates: 10^{-2}, 10^{-3} and 10^{-4} s^{-1}. The cylindrical specimens were extracted from the slab near the upper and lower shells were highest constraints and crack probabilities are found. These tests have been achieved with a TREBEL testing machine equipped with an atmosphere controlled chamber (vacuum or argon), the samples being heated by induction.

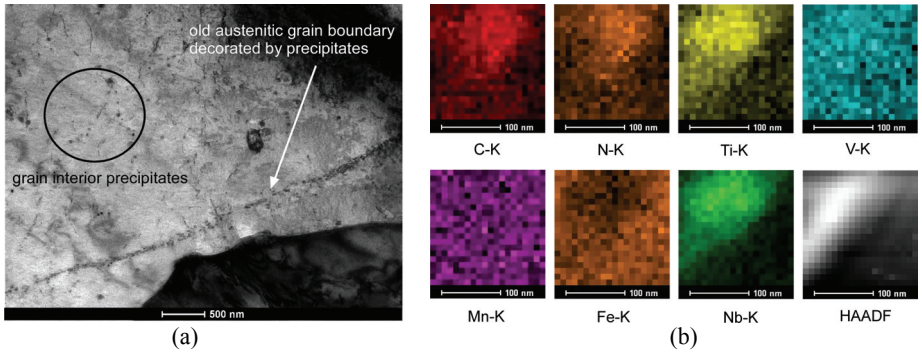

FIGURE 1: Grade C steel: (a) illustration of the localization of the precipitates and (b) STEM map of one inclusion (only the K-ray of each element is illustrated)

In order to correctly test the material in conditions close to the CC process, a three step thermal path was used for the tensile test. The first step consists in the heating of the sample and to its maintain at a annealing temperature of 1350°C during 10 minutes to recover the original microstructure (i.e. austenitic grains with no precipitates) found in the material during the first moment of the CC. Then, the second step consists to decrease the temperature to the test temperature with a cooling rate close to the CC one (around 60°/min [4]). Finally, during the last step, the tensile test is performed once the temperature has been homogenized in the specimen.

Description of the Model

The objective of the numerical study is to predict the crack appearance within a representative mesoscopic cell submitted to the thermo-mechanical loading happening within the process. The macroscopic thermal stress and strain fields are computed by Lagamine FE model. This multi-scale model is employed. This model reproduces the macroscopic rheological behaviour of the material and the intergranular damages. Due to the size of the CC slab, to the localization of the cracks and to save computation time, simulations are performed in two steps following the work of Castagne [10,12]. The first step consists in performing a simulation of CC process without damage consideration to predict the thermo-mechanical fields. A Norton-Hoff creep like constitutive law (see equation 1) is then used. During this step, the evolutions of the stress and strain states for the critical area for crack appearance, i.e. near the notch bottom, are recorded. The second step is linked to the damage prediction. To simulate the crack occurrence, simulations are performed with a representative volume element cell loaded as the critical area for crack appearance. This representative cell is formed by a cell of 2x2 mm² embedded in a transition zone as illustrated in figure 2. For the cell, grains are physically introduced with 2D finite elements linked to the core of grains [7] and 1D finite elements linked to the grain boundaries [8]. The cell is loaded by applying the stress and strain state, extracted from the first step, to the transition zone. The transition zone allows getting a homogeneous stress and strain field around the cell. So it is possible to know quite precisely the stress and strain fields in the cell and to compare them to the macroscopic values occurring within the process.

$$\sigma_e = \varepsilon_e^{p_4} \cdot \exp(-p_1 \varepsilon_e) \cdot p_2 \cdot \sqrt{3} \cdot (\sqrt{3} \cdot \dot{\varepsilon}_e)^{p_3} \quad (1)$$

Inside the cell, the mechanical behaviour of the grain core is modelled thanks to the Norton-Hoff creep law. The grain boundaries are modelled by a damage law that takes into account the cavitation and the sliding of the grain boundaries. Both the interface finite elements and the constitutive including parameters linked to the presence of inclusions and voids allow the modelling of the grain boundaries. In this law the damage parameter is explicitly defined. This law follows the cracking of the cell and determines crack appearance occurring through the mechanism

of voids nucleation, growth and coalescence at high temperature. In this damage law, the cavity size and the distance between cavities are the guiding parameters for the calculation of the different state variables occurring in the damage equations. More details about the characteristics of the cell, the mesh and the constitutive law can be found elsewhere [9,10].

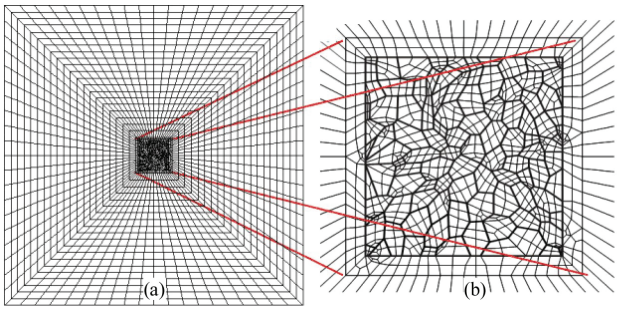

FIGURE 2: Representative cell (a) transition zone + cell and (b) cell

IDENTIFICATION PROCESS

The four parameters of the Norton-Hoff law (i.e. p_1, p_2, p_3 and p_4) have been identified thanks to the simulations without damage of a first series of experimental HTT for temperatures between 900 and 1100°C and various strain rate (i.e: 10^{-3}, 10^{-2} and 5.10^{-2} s^{-1}). The experimental results revealed that the rheological behaviours of the grade A and B are very close and, thus, the same parameters of the Norton-Hoff law were used for these two grades. The comparison between the simulations obtained with the identified set of parameters and the experiments for the grade C is presented in figure 3(a). The results presented in this figure correspond to tensile tests for 1000°C and the three strain rates. Despite differences of flow stress level between the experiments and the simulations, the model predicts in a satisfying way the rheological behaviour.

In order to determine the damage parameters of the law presented before that enable the intergranular fracture, it is necessary to locate the ductility drop so that the tests could be performed at the weak temperatures. Figure 3(b) shows the evolution of necking as a function of the test temperature for unnotched specimens of the three grades strained at 10^{-3} s^{-1}. For these specimens, the ductility drop seems to appear for temperatures between 950 and 750°C. These critical temperatures are not affected by a change of the strain rate and of the stress state as shown by additional tensile tests with various strain rates and notch radii. Consequently, the identification of the damage law must be achieved with a second tensile test series performed for this temperature window. The latter has been adapted for each grade taking into account the scatter of the data: 700-900°C for **grade A**, for 850-950°C for **grade B** and 750-950°C for **grade C**.

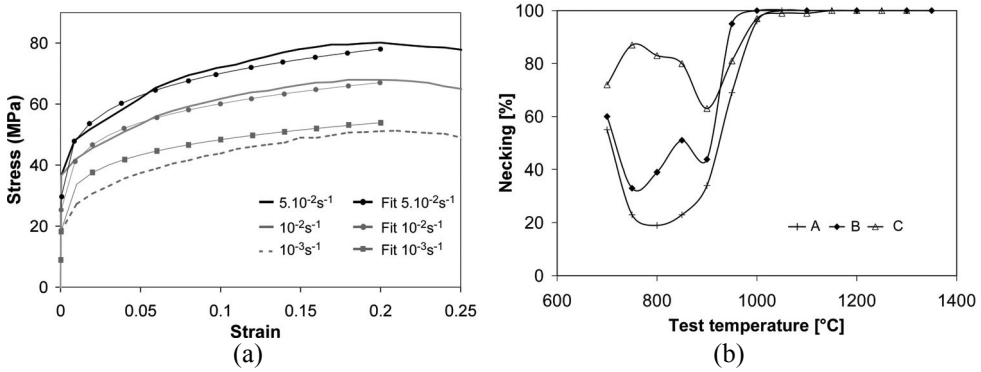

(a) (b)

FIGURE 3: (a) Comparison between the experiments and the simulations of a tensile test of the **grade C** at 1000°C and (b) Evolution of necking for the three grades as a function of the temperature for unnotched samples

For this second series of HTT, three strain rates, i.e. 10^{-2}, 5.10^{-3} and 10^{-3} s^{-1} (this latter being the lowest value possible of the experimental tensile machine) were employed to be close to the real condition of the CC ($\dot{\varepsilon}=10^{-4}$ s^{-1}). The notch radius has also been varied to modify the stress state. Between 7 and 9 configurations (set of T°, strain rate and R) are available for the identification of the damage law depending on the steel grade.

Among the 15 physical parameters of the damage law (see [9]), those linked to the grain boundary sliding (5 parameters) have been set up by the mean grain size computation, by SEM and from the work of Nee [11]. Three others parameters linked to the FE computations were extracted form the work of Castagne [12]. The remaining 7 parameters are related to the damage by void nucleation, growth and coalescence. The initial cavity size, interdistance and angle were obtained thanks to the TEM analysis of the precipitates. The last parameters are linked to the cavity density, the nucleation process and fracture and must be obtained by a proper identification process using the second tensile test series described above. The identification has been done for each grade by searching the set of parameters which give the best prediction for the different tensile configurations.

Figure 5 represents the comparison between the experiments and the simulations for the rheological behavior and the fracture displacement for **grade B**. The load displacement curve is computed by a macroscopic FE element model. The local stress-strain curve at the root of the notch is then applied at the mesoscopic cell model which predicts the crack events. Experimentally, the fracture is reached when an inflexion point is found at the end of the tensile curve. In figure 4 case, fracture occurs experimentally around 11.75 mm while the prediction is around 11 mm. As shown in table 3, the error between the predicted fracture and the experiment for this grade is less than 15% which is satisfying taking into account the low reliability of the experimental determination of fracture. The poor number of experiments did not allow the computation of the experimental error. For the two others grades, the agreements between the experiments and the simulations are less convincing. For these cases, the maximal error is around 50% for a given tensile configuration.

The mesoscopic model developed in this study is hence able to predict the rheological behavior and the damage for the three grades with an error which depends on the material. The microstructural investigation of the different samples may partially explain the differences of prediction. The TEM study revealed that except for the grade B, precipitates are found in the grain boundaries of the austenite and inside the grains. Even if the density of precipitates is lower in the grain interior than in the grain boundaries, the probability that damage occurs in a transgranular way cannot be neglected. This kind of damage is not taken into account in the mesoscopic model and could explain some of the differences for **grade A** and **C**. A sensitivity analysis of the damage constitutive law reported that the model is sensitive to the microstructural parameters (cavity size, interdistance and density)[9]. The identification of these damage parameters from microstructural measurements of the grain size and of the precipitates may be erroneous due to the low number of grains and precipitates analyzed which may induce a significant error. The parameters defining the cavity size and the interdistance are constant within the mesoscopic cell when they should be varied along grain boundaries as observed in reality. Crack event probably results from localized events that the model does not take enough into consideration. New analysis of the austenitic grain size using a large value of grains and a new investigation of the precipitates distribution should be performed to ensure accurate values for the damage law parameters. Heterogeneous damage parameters within the cell should be performed.

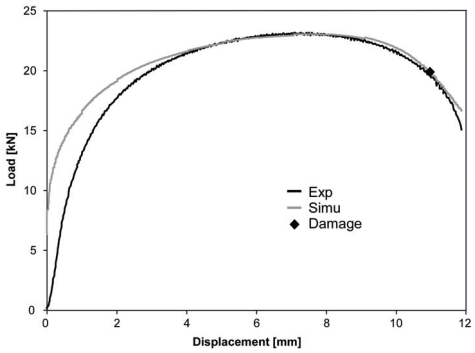

FIGURE 4: Comparison between the experiments and the simulations of a tensile test of the **grade B** at 850°C, R=2 mm and strain rate = 0.01 s^{-1}.

TABLE 3. Comparison between the experimental and predicted critical displacement for fracture for Grade B

T (°C)	Strain rate (s^{-1})	R (mm)	D_{exp} (mm)	D_{num} (mm)	Error (%)
850	0.01	2	11.75	11.00	1.42
850	0.005	2	9.06	10.49	10.78
850	0.001	2	9.97	8.79	6.87
900	0.01	2	11.13	11.34	1.88
900	0.005	2	11.24	10.87	3.31
900	0.001	2	9.1	9.26	1.80
950	0.01	2	12.02	12.64	5.15
950	0.005	2	11.96	12.01	0.38

The systematic comparison of the predicted and experimental values for fracture displacement for the three grades show that the predicted value is generally lower that the experimental one. Numerically, fracture is detected when the fracture criterion is reached on one integration point. Experimentally, fracture is detected from an inflexion point on the tensile curve. This macroscopical inflexion point must result from various damage events in the material as only one fracture event cannot be detected as for the simulations. A better determination of the fracture moment for the experiments by non-destructive control techniques such as acoustic emission must be employed to check the validity of the model. Work is still in progress

CONCLUSIONS

The results presented in this paper show that a multi-scale model for crack formation prediction is ready to be used for the prediction of the fracture during continuous casting. The differences between the experiments and the simulations within the model identification step proceed from various issues which have to be solved to allow industrial use of this model.

ACKNOWLEDGMENTS

The authors acknowledge the Interuniversity Attraction Poles Programme of Belgium (Contract P6/24), the Belgian Fund for Scientific Research and the industrial partners (Arcelor, Industeel, Carinox and IEHK). Professor Senk of the RWTH University is also greatly acknowledged for his help on the hot tensile tests. The Walloon Region is also acknowledged.

REFERENCES

1. H. Suzuki, S. Hishimura, J. Imamura and Y. Nakamura, *Transaction ISIJ* **24**, 169-177 (1984)
2. J.K. Brimacombe and K. Sorimachi, *Metallurgical Transactions B* **8**, 489-505 (1977)
3. F. Pascon, S. Cescotto and A.M. Habraken, *Int. J. Numer. Meth. Engng* **1**, 1-34 (2005)
4. B. Mintz, S. Yue and J.J. Jonas, *Int. Mater. Review* **36**, 187-217 (1991)
5. B. Mintz, A. Cowley, R. Abushosha and D.N. Crowther, *Mat. Sci. Tech*. **15**, 1179-1185 (1999)
6. Z. Mohamed, *Mat. Sci. Eng.* **A326**, 255-260 (2002)
7. Y.Y. Zhu and S. Cescotto, *Int. J. Num. Meth. Engrg*, **38**, 685-716, (1995)
8. A.M. Habraken and S. Cescotto *Mathl. Comput. Modelling*, **28** 153-169 (1998)
9. R. Schwartz, S. Castagne and A.M. Habraken, *Comp. Meth. Mat. Sci.* **7**, 237-242, (2007)
10. S. Castagne, M. Remy and A.M. Habraken, *Key. Eng. Mater***. 223**, 145-150 (2003)
11. A. Needleman and J.R. Rice, *Acta Metallurgica* **28**, 1315-1332 (1980)
12. S. Castagne, D. Talamona and A.M. Habraken*, Int. J. Form. Proc*.**10**, 23-43 (2007)